JOURNAL OF AEROSOL MEDICINE
Volume 1, Number 1, 1988
Mary Ann Liebert, Inc., Publishers

Deposition of Inhaled Fibrous Particles in the Human Lung

B. ASGHARIAN and C.P. YU

Department of Mechanical and Aerospace Engineering, State University of New York at Buffalo, Amherst, NY 14260

ABSTRACT

A theoretical model was developed to calculate the deposition of inhaled fibrous particles in the human lung. In the derivation of deposition formulae, the simultaneous effects of the velocity shear in the air flow and Brownian rotation on particle orientation were considered. Total deposition of fibers in the lung at mouth breathing was found to be smaller than that of spherical ones with the same mass, and deposition in the lung at nose breathing showed considerably lower deposition than that at mouth breathing. Calculated deposition in the alveolar region of the lung from this model compared favorably with the postmortem data.

INTRODUCTION

Deposition of fibrous particles in the human respiratory tract is a very complicated process because of the sequential branching of the airway passages, the change in the orientation of individual passages, and the complex behavior of long fibrous particles in this system. There are only a few theoretical studies made to date which address this problem. Beeckmans (1972) extended the deposition results of spherical particles to fibrous ones by assuming that the particles were randomly oriented in the airways at all times. He showed that the deposition result for fibrous particles could not be derived directly from that for spherical ones by means of an equivalent spherical particle diameter because this diameter differs depending on the mechanism of deposition. Further, in Beeckmans' analysis, particle removal from the nasopharyngeal air stream and interception deposition at the bifurcation sites were neglected. These loss mechanisms are important for large and long fibers.

Another very extensive deposition model for fibrous particles was developed by Harris and Fraser (1976), using existing and new formulae for calculating the deposition of fibrous particles in an airway due to different mechanisms. The particles were assumed to be oriented either with their major axes along the flow or randomly in space, depending upon the flow condition and the strength of particle Brownian motion. They also derived a deposition formula in the nasopharynx by considering impaction deposition and interception deposition by nasal

Keywords: Fiber, deposition, human lung

hairs. Both Beeckmans and Harris calculated total and regional deposition in humans using the lung model of Weibel (1963).

In this paper, we further extend the studies of Beeckmans and Harris on the deposition model for fibrous particles in the human lung by performing a detailed analysis of particle orientation in each generation of the airway. It is known that fibrous particles are subjected to a combined translational and rotational motion. The particle rotation is caused by the velocity gradient in the flow (Jeffery, 1922) and by Brownian motion. Both these effects are considered in the derivation of new deposition formulae in an airway. A procedure is also developed and utilized to allow a smooth transition from the velocity gradient dominated particle rotation to the one controlled by Brownian motion. The regional and total deposition are then calculated and compared with experimental data.

COLLECTION EFFICIENCIES IN AIRWAYS

Deposition of fibrous particles in an airway is strongly related to the orientation of particles with respect to the direction of the air flow. There are two mechanisms which determine the particle orientation: the velocity shear of the flow and Brownian rotation. At any time t, the orientation of particles, expressed by an orientation distribution function, $P(\phi,\theta,t)$ is governed by the Fokker-Planck equation

$$\frac{\partial P}{\partial t} + \nabla.(\vec{\omega}P - {}^{r}D\nabla P) = 0 \tag{1}$$

and

$$\int_0^{2\pi}\int_0^{\pi/2} P(\phi,\theta,t)\sin\theta d\theta d\phi = 1 \tag{2}$$

where $\vec{\omega}$ is the angular velocity of particle rotation, ${}^{r}D$ is the Brownian diffusion coefficient for rotation, and ϕ and θ are the Eulerian angles shown in Fig. 1.

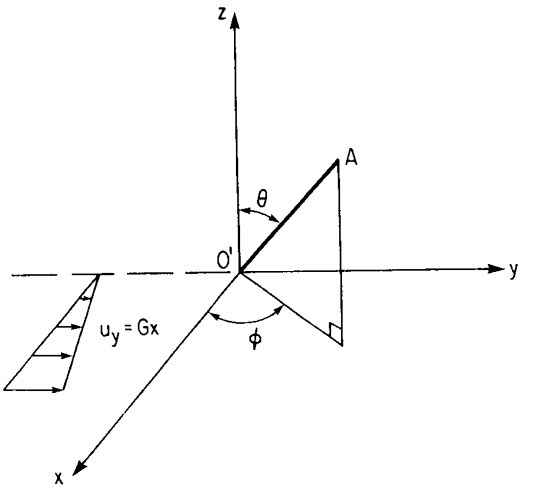

FIGURE 1. Orientation of a Fibrous Particle.

Fibrous particles deposit on the airway surface by various mechanisms including diffusion, sedimentation, impaction and interception. The deposition efficiencies for the first three mechanisms have been derived for spherical particles. Each of these results can be extended to fibrous particles by considering orientation effects in the manner described below.

The diffusion efficiency of spherical particles in a parabolic flow was obtained by Ingham (1975) in the form

$$\eta_d = \{1-0.819 \exp(-14.63\Lambda) -0.097 \exp(-89.22\Lambda) -0.0325 \exp(-228\Lambda) -0.0509 \exp(-125.9\Lambda^{2/3})\} \quad (3)$$

where

$$\Lambda = \frac{L\,{}^tD}{4UR^2} \quad (4)$$

in which L and R are, respectively, the airway length and radius, U is the average velocity in the airway, and ${}^tD$ is the translational diffusion coefficient of particles. Equation (3) can be applied to fibers if a proper expression for ${}^tD$ is used. Asgharian et al. (1987) have derived the following expression for ${}^tD$

$$ {}^tD = kT \int_{r^*=0}^{1} \int_{\phi=0}^{2\pi} \int_{\theta=0}^{\pi/2} \frac{C_F(d_e)P(r^*,\phi,\theta)}{f^o} \sin\theta d\theta d\phi\, dr^* \quad (5)$$

where $P(r^*,\phi,\theta)$ is the orientation distribution function of particles at steady state, k is the Boltzmann constant, T is the absolute temperature, $r^* = r/R$ with r being the radial distance from the axis of the airway, f^o is the drag per unit velocity in the continuum regime, and C_F is the Cunningham correction factor given by

$$C_F = 1 + Kn\left[A + B\exp(-\frac{C}{Kn})\right] \quad (6)$$

In equation (6), A, B and C are constants with A=1.142, B=0.558 and C=0.999 for solid particles (Allen and Raabe, 1985), and Kn is the Knudsen number defined by

$$Kn = \frac{2\lambda}{d_e} \quad (7)$$

where λ is the mean free path of the gas molecules and d_e is the equivalent diameter for the slip correction, determined from the expression

$$\frac{d_e}{d_f} = \frac{1.7 d_f \beta(\frac{\cos^2\psi_d}{d_{f\perp}} + \frac{\sin^2\psi_d}{d_{f\parallel}})}{6\pi\,(\frac{\cos^2\psi_d}{11.18} \quad \frac{\sin^2\psi_d}{4.59})} \quad (8)$$

in which d_f and β are, respectively, the particle minor diameter and the aspect ratio, and ψ_d is the diffusion angle, defined as the angle between the particle polar axis and the axis of the airway.

The collection efficiency for spherical particles due to sedimentation in a horizontal tube was derived by Pich (1972). It has the following expression

$$\eta_s = \frac{2}{\pi}(2\varepsilon\sqrt{1-\varepsilon^{2/3}} - \varepsilon^{1/3}\sqrt{1-\varepsilon^{2/3}} + \sin^{-1}\varepsilon^{1/3}) \quad (9)$$

where

$$\varepsilon = \frac{3u_g L}{8UR} \quad (10)$$

in which u_g is the particle terminal settling velocity. In an inclined airway

with an inclination angle γ, equation (10) is modified by replacing u_g with $u_g \cos\gamma$. For a single fiber which makes an angle ψ_s with the horizontal, the terminal settling velocity can be found as follows:

$$u_g = \frac{\rho g d_f^3 \beta C_F(d_e)}{18\mu} \left(\frac{1}{d_{f||}} \sin^2\psi_s + \frac{1}{d_{f\perp}} \cos^2\psi_s \right) \tag{11}$$

where ρ is the particle density, g is the gravitational constant, μ is the absolute viscosity of the air, and $d_{f||}$ and $d_{f\perp}$ are, respectively, the stokes diameters for the cases with the particle polar axis parallel and perpendicular to the direction of motion. The stokes diameter is defined as the diameter of a sphere which has the same drag as the particle in the continuum regime. Oseen (1927) obtained expressions for d_f and d_f as follows:

$$d_{f||} = \frac{\frac{4}{3}(\beta^2-1)d_f}{\frac{2\beta^2-1}{\sqrt{\beta^2-1}} \ln(\beta+\sqrt{\beta^2-1})-\beta} \tag{12}$$

$$d_{f\perp} = \frac{\frac{8}{3}(\beta^2-1)d_f}{\frac{2\beta^2-3}{\sqrt{\beta^2-1}} \ln(\beta+\sqrt{\beta^2-1})+\beta} \tag{13}$$

A descending particle at its terminal velocity experiences a constant force exerted on it while its velocity and orientation keep changing as a result of rotation. The average settling velocity of a particle is therefore

$$\bar{u}_g = \frac{2}{\pi} \int_{\alpha=0}^{\pi/2} \int_{r^*=0}^{1} \int_{\phi=0}^{2\pi} \int_{\theta=0}^{\pi/2} u_g(\phi,\theta) P(r^*,\phi,\theta) \sin\theta d\theta dr^* d\alpha \tag{14}$$

where α is the angle between the horizontal line and the line connecting the center of the particle to the center of an airway cross section. Upon substitution of equation (14) for u_g in equation (10), the average sedimentation efficiency of fibrous particles in randomly oriented airways can be obtained as follows:

$$\bar{\eta}_s = \int_{\gamma=0}^{\pi/2} \eta_s(\gamma) \cos\gamma d\gamma \tag{15}$$

Impaction efficiency is the fraction of particles deposited at the bifurcation of an airway due to their inertia. At small particle stokes numbers. Chan and Yu (1981) obtained the impaction efficiency for spherical particles in the following simple form using a bend model:

$$\eta_{imp} = 0.768 \ St \ \theta_b \tag{16}$$

where θ_b is the bend angle and St is the Stokes number which represents particle's inertia. The above expression can be extended to fibers if one uses the average Stokes number over different orientations of fibrous particles. The Stokes number for a single fiber which makes an angle of ψ_i with the axis of the parent tube of a bifurcating airway has the following form:

$$St = \frac{\rho d_f^3 \beta U C_F}{18\mu R(d_{f||}\sin^2\psi_i + d_{f\perp}\cos^2\psi_i)} \tag{17}$$

The average of the Stokes number is then

$$\overline{St} = \int_{r^*=0}^{1} \int_{\phi=0}^{2} \int_{\theta=0}^{\pi/2} St(\phi,\theta) P(r^*,\phi,\theta) \sin\theta d\theta d\phi dr^* \tag{18}$$

Upon substitution of $\overline{St}$ from equation (18) into (16) for St, the impaction efficiency of fibers in a bifurcating airway is obtained.

Because of their elongated geometry, fibers also deposit at the carina of a bifurcation due to interception. An expression for the interception efficiency of fibrous particles, was derived by Asgharian (1988) as follows:

$$\eta_{int} = \frac{1}{2\pi} \int_{\phi=0}^{2\pi} \int_{\theta=0}^{\pi/2} I(\phi,\theta) \sin\theta d\theta d\phi \tag{19}$$

$$I(\phi,\theta) = \frac{8}{\pi} \int_{\Gamma=0}^{\Gamma'} \int_{r^*=0}^{\frac{\ell_p \sin(\Gamma-\Omega)}{2R\cos\Gamma}} P(r^*,\phi,\theta) r^*(1-r^{*2}) dr^* d\Gamma$$

$$+ \int_{\Gamma=\Gamma'}^{\pi/2} \int_{r^*=0}^{r^{*\prime}} P(r^*,\phi,\theta) r^*(1-r^{*2}) dr^* d\Gamma \tag{20}$$

where

$$\Gamma' = \cos^{-1}\left(\frac{\ell_p}{2R} \cos\Omega\right) \tag{21}$$

$$\ell_p = \ell_f (1-\sin^2\theta\sin^2\phi)^{1/2} \tag{22}$$

$$\Omega = \cos^{-1}\left(\frac{\ell_f \cos\theta}{\ell_p}\right) \tag{23}$$

$$r^{*\prime} = \frac{\ell_p \sin(\Gamma' - \Omega)}{2R\cos\Gamma'} \tag{24}$$

in which ℓ_f and ℓ_p are, respectively, the particle length and its projection on the airway cross-sectional plane.

In order to evaluate the collection efficiencies due to different mechanisms in an airway, an expression for $P(r^*,\phi,\theta)$ is needed. Peterlin (1938) considered the problem of suspended ellipsoidal particles in a uniform flow with constant shear. He solved the Fokker-Planck equation (1) to obtain

$$P(\phi,\theta) = \frac{1}{2\pi}\left\{1 + \frac{3\Delta\sin^2\theta}{6\left(1+\left(\frac{6}{r_{Pe}}\right)^2\right)}\left(-\frac{1}{2}\cos 2\phi + \frac{3}{r_{Pe}}\sin 2\phi\right) + \frac{\Delta^2}{6\left(1+\left(\frac{6}{r_{Pe}}\right)^2\right)} \times \right.$$

$$\left[-\frac{3}{14}(3\cos^3\theta - 1) + \frac{9}{560}(35\cos^4\theta - 30\cos\theta + 3) + \frac{15\sin^4\theta}{100\left(16\left(1+\frac{6}{r_{Pe}^2}\right)\right)} \times \right.$$

$$\left.\left.\left(\cos 4\phi\left(1 - \frac{60}{r_{Pe}^2}\right) - \frac{16}{r_{Pe}}\sin 4\phi\right)\right] + \Delta^3 [\ldots]\right\} \tag{25}$$

where

$$\Delta = \frac{\beta^2 - 1}{\beta^2 + 1} \tag{26}$$

and ^{r}Pe is the rotational Peclet number, defined by

$$^{r}Pe = \frac{G}{^{r}D} \tag{27}$$

in which G is the velocity gradient, and ^{r}D is the rotational diffusion coefficient, given by

$$^{r}D = B_{\omega} kT \tag{28}$$

In equation (28), B_{ω} is the angular mobility of the fiber about the axis of rotation. For a prolate ellipsoid of revolution, it was found that (Gans, 1928)

$$B_{\omega} = \frac{3\left[\frac{2\beta^2-1}{\sqrt{\beta^2-1}}\ell n(\beta+\sqrt{\beta^2-1})-\beta\right]}{2\pi\mu d_f^3(\beta^4-1)} \tag{29}$$

Equation (25) can be applied locally to a parabolic flow in a tube for which the velocity gradient is a function of the radial position. Since equation (25) is a serious solution of Δ, a rapid convergence of this equation requires $\Delta<<1$, which corresponds to small values of β. However, for fibers with large β, Δ approaches unity and many terms in equation (25) are needed in order to assure an accurate result. To avoid this difficulty, an alternative approach becomes necessary in calculating collection efficiencies.

We assume that the collection efficiency of particles by each deposition mechanism is a linear combination of two separate efficiencies, one for the case of random particle orientation and other for the particle orientation as determined from the periodic rotation of particles resulting from the velocity shear, i.e.,

$$\eta = A_1 \eta_P + A_2 \eta_R \tag{30}$$

where η_P and η_R are, respectively, the collection efficiencies of particles in periodic rotation and random orientation, and A_1 and A_2 are coefficients given by the expressions

$$A_1 = \frac{^{r}Pe^{*}}{^{r}Pe^{*}+ 50} \tag{31}$$

$$A_2 = \frac{50}{^{r}Pe^{*}+50} \tag{32}$$

where

$$^{r}Pe^{*} = \frac{u}{R\,^{r}D} \tag{33}$$

The numerical value of 50 in equations (31) and (32) was obtained by matching solution (30) with the exact solution presented above for $^{r}Pe^{*}<<1$, in which P was calculated from equation (25). Equation (30) also implies that the orientation distribution function has the same linear combination form. The orientation distribution function for the velocity shear dominated case is calculated numerically from the theory of Jeffery (1922).

The total deposition efficiency of particles in an airway per unit length of airway is obtained by summing the efficiencies of all deposition mechanisms. That is,

$$\eta_{total} = \bar{\eta}_s + \eta_{imp} + \eta_d + \eta_{int} \tag{34}$$

Figures 2 to 4 show the deposition efficiencies of each individual mechanism in various airway generations of Weibel's lung model at a flow rate of 375 cm^3/sec for different equivalent mass diameters d_{em}($d_{em} = d_f \beta^{1/3}$ for an ellipsoidal particle of unit density). The results show that for very small particles (d_{em} = 0.01 μm), only diffusion is important and the deposition efficiency increases with

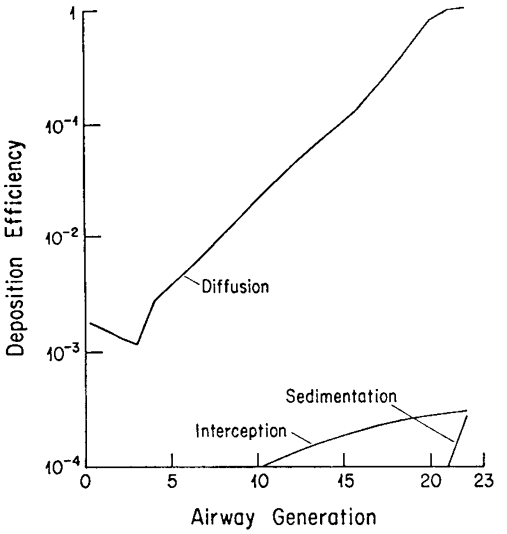

FIGURE 2. Deposition Efficiency of Fibers in Different Generations of the Weibel Lung Model at a Flow Rate of 375 cm^3/sec for d_{em} = 0.01 μm and Unit Density.

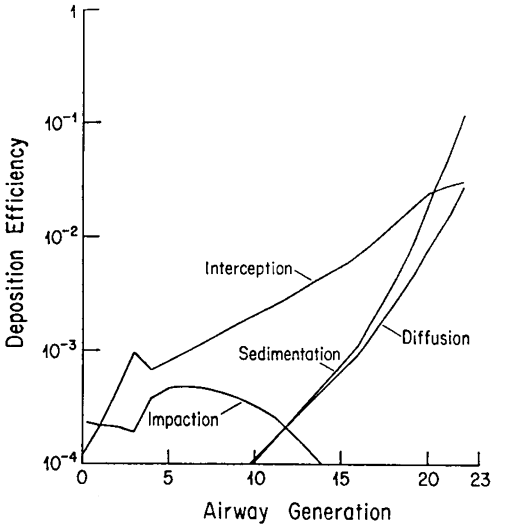

FIGURE 3. Deposition Efficiency of Fibers in Different Generations of the Weibel Lung Model at a Flow Rate of 375 cm^3/sec for d_{em}= 1 μm and Unit Density.

generation number because of the slower flow rate and larger residence time for diffusion. For particles with d_{em} = 1 μm, interception deposition is the most

important mechanism at almost all airway generations except in the very deep lung where sedimentation dominates. Also, for very large particles (d_{em} = 10 μm), the impaction efficiency is the highest in the earlier generations and sedimentation is highest in the later generations. Based on these results, one can deduce that in the upper airways, impaction and interception, and in the deeper airways interception, diffusion and sedimentation are the effective deposition mechanisms in the lung.

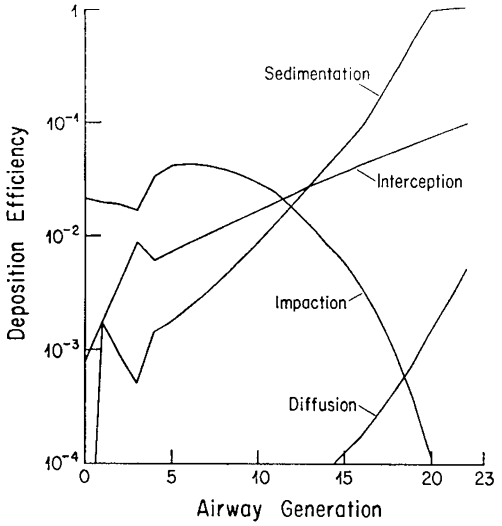

FIGURE 4. Deposition Efficiency of Fibrous in Different Generations of the Weibel Lung Model at a Flow Rate of 375 cm^3/sec for d_{em}=10 μm and Unit Density.

COLLECTION EFFICIENCIES IN THE NOSE AND MOUTH

Particles also deposit in the head region by impaction and interception. In the mouth, impaction is the only important deposition mechanism, while in the nose, nasal hairs contribute to interception deposition. The expressions for impaction deposition in the nose and mouth have been obtained for spherical particles by Yu et al. (1981). These expressions are modified for fibrous particles by again using the average stokes number over all particle orientations. However, due to the large air velocity in the head region, particles are assumed to have random orientation at all times.

For the interception deposition of fibrous particles due to the nasal hairs in the nostril, simple analytical expressions were derived by Asgharian (1987). These expressions are

$$N_{int} = 0.921\ [1-(1-24\ \ell_f)^7], \quad \text{for } \ell_f < 0.035\text{cm} \tag{35}$$

$$N_{int} = 0.921, \quad \text{for } \ell_f > 0.035\text{cm} \tag{36}$$

where ℓ_f is the fiber length in cm.

The total deposition efficiency in the nose is determined by combining impaction and interception. Assuming that these mechanisms are independent, the total deposition efficiency in the nose is given by

$$N = 1-(1-N_{imp})(1-N_{int}) = N_{imp} + N_{int} - N_{imp}\,N_{int} \tag{37}$$

TOTAL AND REGIONAL DEPOSITION

The collection efficiencies derived for the airways and for the head region are used in a deposition model to calculate the deposition of fibers in the human respiratory tract based upon Weibel's symmetric lung model. The lung volume is taken to be 3000 cm^3, the tidal volume is 750 cm^3 and the breathing period is 4 seconds, which includes 1.74 seconds for inhalation, 0.2 seconds for pause, and 2.06 seconds for exhalation. The deposition results for mouth and nose breathing are plotted in Figs. 5-11.

The tracheobronchial deposition of particles through mouth breathing is shown in Fig. 5. For small particles with equivalent mass diameter $d_{em} < 0.1$ μm, diffusion deposition is dominant and a larger aspect ratio of the particle results in a lower deposition. For d_{em} between 0.1 μm and 1 μm, diffusion, impaction and interception are all present and there is no clear relationship between the aspect ratio of the particle and the amount of deposition. For $d_{em} > 1$ μm, diffusion becomes unimportant and the deposition curves for different aspect ratios cross each other and one cannot identify a dominant deposition mechanism. Hence, deposition in the tracheobronchial region can be categorized into three regions: a diffusion dominated region for d_{em} less then 0.1 μm, a transition region in which impaction, interception and diffusion all contribute to deposition, and an interception-impaction region for d_{em} larger than 1 μm. The mechanism of sedimentation is less important in the tracheobronchial region for large particles because of the smaller residence time, as shown in Figs. 3 and 4.

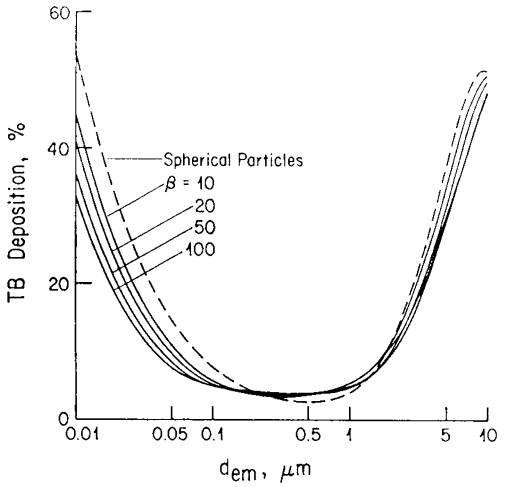

FIGURE 5. Tracheobronchial Deposition of Unit Density Fibers via Mouth Breathing in the Weibel Lung Model at a Lung Volume of 3000 cm^3, a Tidal Volume of 750 cm^3, and a Breathing Frequency of 15 cycles/min.

Figure 6 shows the results of alveolar deposition via mouth breathing. Since the deposition in the alveolar region is affected by both the filtering effect of the tracheobronchial region and the deposition efficiency of the alveolar region, the results are more complicated than those in the tracheobronchial region. For extremely small particles ($d_{em} < 0.02$ μm) and very large particles ($d_{em} > 5$ μm), the filtering effect is important due to diffusion and interception respectively in the tracheobronchial region. Between $d_{em} = 0.02$ μm and $d_{em} = 5$ μm, the alveolar deposition is controlled by diffusion from 0.02 μm to 0.5 μm and by sedimentation from 0.5 μm to 5 μm. Increasing the aspect ratio of the particle in this size range results in a decrease in deposition. A plot of the total deposition (sum of the head, tracheobronchial and alveolar deposition) via mouth breathing is shown in Fig. 7. The results show that particles with lower aspect ratios normal-

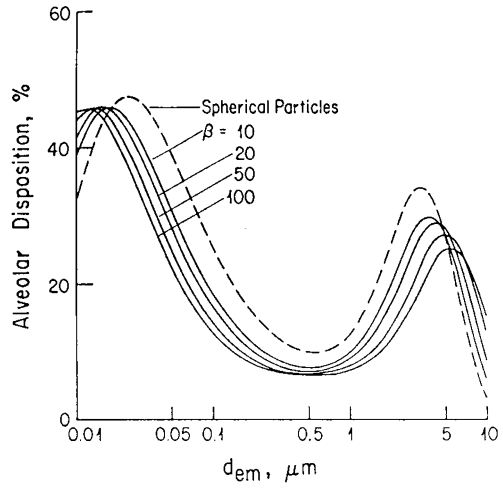

FIGURE 6. Alveolar Deposition of Unit Density Fibers via Mouth Breathing in the Weibel Lung Model at a Lung Volume of 3000 cm^3, a Tidal Volume of 750cm^3, and a Breathing Frequency of 15 cycles/min.

ly have higher total deposition. This implies that the decreases in deposition by the combined mechanisms of diffusion, sedimentation and impaction resulting from a thinner and longer particle outweigh the increase in interception deposition in most cases.

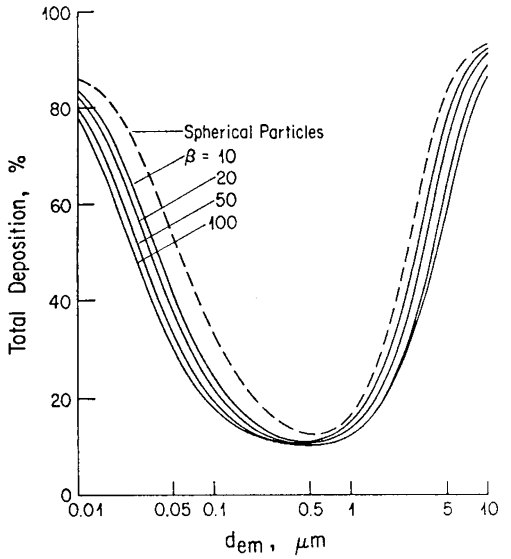

FIGURE 7. Total Deposition of Unit Density Fibers via Mouth Breathing in the Weibel Lung Model at a Lung Volume of 3000 cm^3 a Tidal Volume of 750 cm^3, and a Breathing Frequency of 15 cycles/min.

The calculated total and regional depositions via nose breathing are plotted in Figs. 8-10. Because of a stronger impaction deposition in the nose and the

contribution of interception deposition from the nasal hairs, the deposition in the tracheobronchial and alveolar region are significantly lower than the results of mouth breathing. Total deposition is also higher for the nose breathing mode.

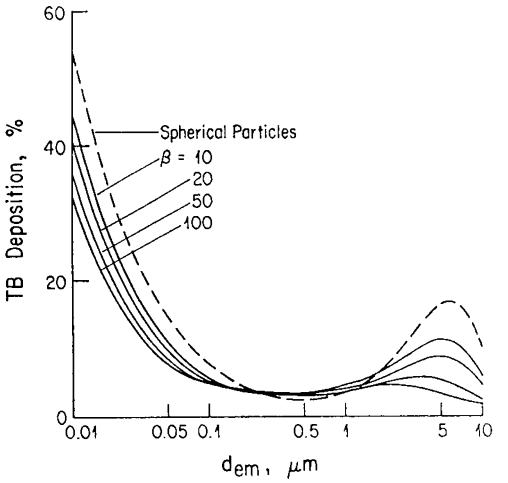

FIGURE 8. Tracheobronchial Deposition of Unit Density Fibers via Nose Breathing in the Weibel Lung Model at a Lung Volume of 3000 cm^3, a Tidal Volume of 750 cm^3, and a Breathing Frequency of 15 cycles/min.

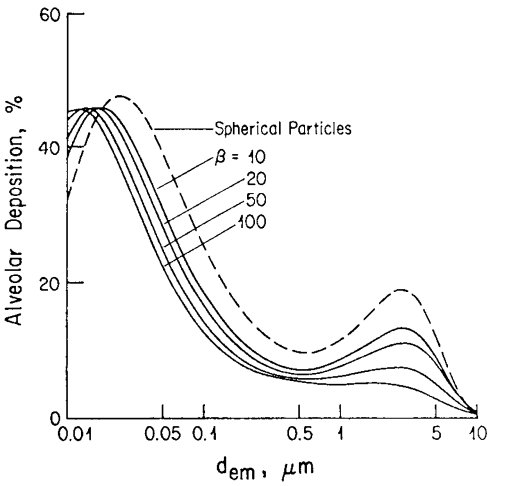

FIGURE 9. Alveolar Deposition of Unit Density Fibers via Nose Breathing in the Weibel Lung Model at a Lung Volume of 3000 cm^3, a Tidal Volume of 750 cm^3, and a Breathing Frequency of 15 cycles/min.

To verify the deposition model of fibers in the human lung, we have made a comparison between the calculated alveolar deposition with data reported by Timbrell (1982). Timbrell studied the distribution of fibers in the lung specimens of former employees and local inhabitants of the Paakkila anthophyllite mine.

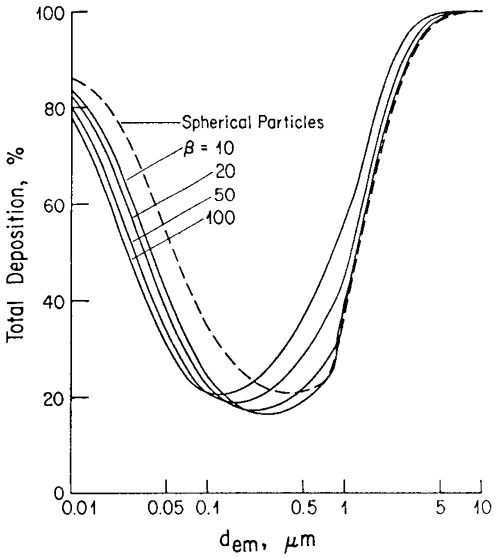

FIGURE 10. Total Deposition of Unit Density Fibers via Nose Breathing in the Weibel Lung Model at a Lung Volume of 3000 cm^3, a Tidal Volume of 750 cm^3, and a Breathing Frequency of 15 cycles/min.

From the data on fiber size distribution and fibers recovered from lung tissues, he obtained a bivariate distribution of fibers retained in the lung. His results for the left upper lobe of a mine worker are shown in Fig. 11. A similar plot based on our calculation is shown in Fig. 12 for a particle density of 3 g/cm^3 which corresponds to these fibers. By comparing Figs. 11 and 12, one can see that both plots show a maximum relative deposition at fiber length of 7 μm, but the corresponding fiber diameters are 0.5 μm in Timbrell's results and 0.75 μm in our calculation. The general pattern of deposition with respect to particle size in two figures, however, is strikingly similar. It should be born in mind that our results are calculated from deposition alone, while Timbrell's results correspond to the retention of fiber in the lung tissues after a long period of exposure which involves clearance mechanisms.

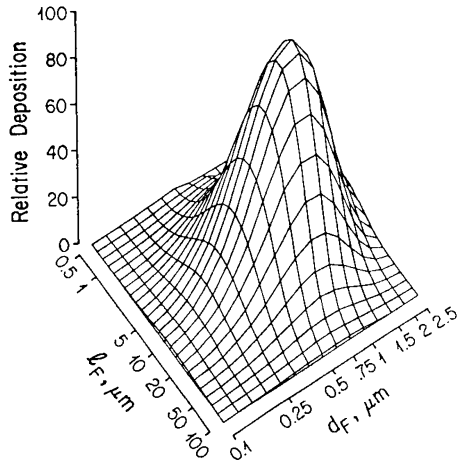

FIGURE 11. Bivariate Presentation of Fiber Retention Obtained by Timbrell (1982) from the Lung Specimens of a Mine Worker.

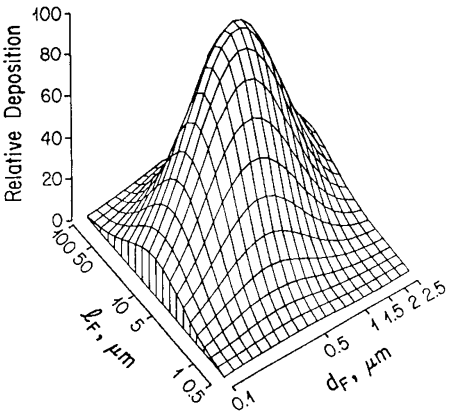

FIGURE 12. Bivariate Distribution of Fiber Deposition in the Alveoli via Nose Breathing Calculated from the Present Theory.

ACKNOWLEDGMENT

This work was supported by Grant No. HL-38503 from the National Heart, Lung and Blood Institute.

REFERENCES

Allen, M.D. and Raabe, O.G. (1985). Slip Correction Measurements of Spherical Solid Aerosol Particles in an Improved Millikan Apparatus. Aerosol Sci. Tech. 4, 269-286.

Asgharian, B. (1988). Theoretical Deposition of Fibrous Particles in the Respiratory Tract of Humans and Rats. Ph.D. Thesis, State University of New York at Buffalo.

Asgharian, B., Yu, C.P., and Gradon, L. (1987). Deposition of Fibers in a Tubular Flow. American Association for Aerosol Research Annual Meeting, September 14-17, Seattle, WA.

Chan, T.L. and Yu, C.P. (1982). Charge Effects on Particle Deposition in the Human Tracheobronchial Tree. Ann. Occup. Hyg. 26, 65-75.

Gans, K.R. (1928). Zur Theories der Brownschen Molekulargewegung. Ann. Physik 86, 628-656.

Harris, R.L., and Fraser, D.A. (1976). A Model for Deposition of Fibers in the Human Respiratory System. Am. Ind. Hyg. Assoc. J. 37, 73-89.

Ingham, D.B. (1975). Diffusion of Aerosols from a Stream Flowing through a Cylindrical Tube. J. Aerosol Sci. 6, 125-132.

Jeffery G.B. (1922). The Motion of Ellipsoidal Particles Immersed in a Viscous Fluid. Proc. Roy. Soc. London A102, 161-179.

Mercer, T.T., Mollow, P.F., and Stober, W. ed. (1972). Assessment of Airborne Particles. C. Thomas, Springfield, IL, p. 361.

Oseen, C.W. (1927). Hydrodynamik. Leipzig, Akademische Verlag.

Peterlin, A. (1938). Uber die Viskositat Von Verdunnten Losungen und Suspensionen in Abhangigkeit Von der Teilchenform. Z. Phys. 111, 232-263.

Pich. J. (1972). Theory of Gravitational Deposition of Particles from Laminar Flows in Channels. J. Aerosol Sci. 3, 351-361.

Timbrell, V. (1982). Deposition and Retention of Fibers in the Human Lung. Ann. Occup. Hyg. 26, 347-369.

Weibel, E.R. (1963). Morphometry of the Human Lung., Academic Press, N.Y.

Yu, C.P. (1978). Exact Analysis of Aerosol Deposition during Steady Breathing. Powder Technology 21, 55-62.

Yu, C.P. Diu, C.K., and Soong, T.T. (1981). Statistical Analysis of Aerosol Deposition on Nose and Mouth. Am. Ind. Hyg. Assoc. J. 42, 726-733.

Yu, C.P., Asgharian, B., and Yen, B.M. (1986). Impaction and Sedimentation Deposition of Fibers in Airways. Am. Ind. Hyg. Assoc. J. 47, 72-77.

Article received October 1, 1987
In final form January 19, 1988
Reviewed by:
T. Myojo

Address reprint requests to:
Dr. C.P Yu, Department of Mechanical and Aerospace Engineering, State University of New York at Buffalo, Amherst, NY 14260.

This article has been cited by:

1. Andriy Roshchenko, Warren H. Finlay, Peter D. Minev. 2011. The Aerodynamic Behavior of Fibers in a Linear Shear Flow. *Aerosol Science and Technology* **45**:10, 1260-1271. [CrossRef]
2. R. Sturm. 2011. Modeling the deposition of bioaerosols with variable size and shape in the human respiratory tract – A review. *Journal of Advanced Research* . [CrossRef]
3. Pramod Kulkarni, Paul A. Baron, Christopher M. Sorensen, Martin HarperNonspherical Particle Measurement: Shape Factor, Fractals, and Fibers 507-547. [CrossRef]
4. B. W. Case, J. L. Abraham, G. Meeker, F. D. Pooley, K. E. Pinkerton. 2011. Applying Definitions of "Asbestos" to Environmental and "Low-Dose" Exposure Levels and Health Effects, Particularly Malignant Mesothelioma. *Journal of Toxicology and Environmental Health, Part B* **14**:1-4, 3-39. [CrossRef]
5. K. E. Duncan, A. J. Ghio, L. A. Dailey, A. M. Bern, E. A. Gibbs-Flournoy, D. J. Padilla-Carlin, V. L. Roggli, R. B. Devlin. 2010. Effect of Size Fractionation on the Toxicity of Amosite and Libby Amphibole Asbestos. *Toxicological Sciences* **118**:2, 420-434. [CrossRef]
6. L MAXIM, J HADLEY, R POTTER, R NIEBO. 2006. The role of fiber durability/ biopersistence of silica-based synthetic vitreous fibers and their influence on toxicology. *Regulatory Toxicology and Pharmacology* **46**:1, 42-62. [CrossRef]
7. Zuocheng Wang, Philip Hopke, Paul Baron, Goodarz Ahmadi, Yung-Sung Cheng, Gregory Deye, Wei-Chung Su. 2005. Fiber Classification and the Influence of Average Air Humidity. *Aerosol Science & Technology* **39**:11, 1056-1063. [CrossRef]
8. R BAAN. 2004. Man-made mineral (vitreous) fibres: evaluations of cancer hazards by the IARC Monographs Programme. *Mutation Research/Fundamental and Molecular Mechanisms of Mutagenesis* **553**:1-2, 43-58. [CrossRef]
9. Thomas J. Lentz, Carol H. Rice, Paul A. Succop, James E. Lockey, John M. Dement, Grace K. LeMasters. 2003. Pulmonary Deposition Modeling with Airborne Fiber Exposure Data: A Study of Workers Manufacturing Refractory Ceramic Fibers. *Applied Occupational and Environmental Hygiene* **18**:4, 278-288. [CrossRef]
10. S Moolgavkar. 2001. The Power of the European Union Protocol to Test for Carcinogenicity of Inhaled Fibers. *Regulatory Toxicology and Pharmacology* **33**:3, 350-355. [CrossRef]
11. L Maxim. 2001. Interspecies Comparisons of the Toxicity of Asbestos and Synthetic Vitreous Fibers: A Weight-of-the-Evidence Approach. *Regulatory Toxicology and Pharmacology* **33**:3, 319-342. [CrossRef]
12. Carol RiceRock Wool and Refractory Ceramic Fibers . [CrossRef]
13. Y.T. DAI, C.P. YU. 1998. Alveolar Deposition of Fibers in Rodents and Humans. *Journal of Aerosol Medicine* **11**:4, 247-258. [Abstract] [PDF] [PDF Plus]
14. Bahman Asgharian, Goodarz Ahmadi. 1998. Effect of Fiber Geometry on Deposition in Small Airways of the Lung. *Aerosol Science and Technology* **29**:6, 459-474. [CrossRef]
15. J. Y. Ding, C. P. Yu, L. Zhang, Y. K. Chen. 1997. Deposition Modeling of Fibrous Particles in Rats: Comparisons with Available Experimental Data. *Aerosol Science and Technology* **26**:5, 403-414. [CrossRef]
16. W Kvasnak. 1996. Deposition of ellipsoidal particles in turbulent duct flows. *Chemical Engineering Science* **51**:23, 5137-5148. [CrossRef]

17. Gerald Vaughan, Sharon Trently. 1996. The toxicity of silicon carbide whiskers, a review. *Journal of Environmental Science and Health, Part A* **31**:8, 2033-2054. [CrossRef]
18. C. P. Yu, L. Zhang, G. Oberdöster, R. W. Mast, D. Maxim, M. J. Utell. 1995. Deposition of Refractory Ceramic Fibers (RCF) in the Human Respiratory Tract and Comparison with Rodent Studies. *Aerosol Science and Technology* **23**:3, 291-300. [CrossRef]
19. Bahman Asgharian, Satish Anjilvel. 1995. The Effect of Fiber Inertia on Its Orientation in a Shear Flow with Application to Lung Dosimetry. *Aerosol Science and Technology* **23**:3, 282-290. [CrossRef]
20. William Kvasnak, Goodarz Ahmadi. 1995. Fibrous Particle Deposition in a Turbulent Channel Flow - An Experimental Study. *Aerosol Science and Technology* **23**:4, 641-652. [CrossRef]
21. C YU, L ZHANG, G OBERDORSTER, R MAST, L GLASS, M UTELL. 1994. Deposition modeling of refractory ceramic fibers in the rat lung. *Journal of Aerosol Science* **25**:2, 407-417. [CrossRef]
22. O BERNSTEIN, M SHAPIRO. 1994. Direct determination of the orientation distribution function of cylindrical particles immersed in laminar and turbulent shear flows. *Journal of Aerosol Science* **25**:1, 113-136. [CrossRef]
23. T. B. Martonen, Y. Yang, Z. Q. Xue. 1994. Effects of Carinal Ridge Shapes on Lung Airstreams. *Aerosol Science and Technology* **21**:2, 119-136. [CrossRef]
24. Bahman Asgharian, Satish Anjilvel. 1994. Inertial and Gravitational Deposition of Particles in a Square Cross Section Bifurcating Airway. *Aerosol Science and Technology* **20**:2, 177-193. [CrossRef]
25. M SHAPIRO, M GOLDENBERG. 1993. Deposition of glass fiber particles from turbulent air flow in a pipe. *Journal of Aerosol Science* **24**:1, 65-87. [CrossRef]
26. IMRE BALÁSHÁZY, TED B. MARTONEN, WERNER HOFMANN. 1990. Fiber Deposition in Airway Bifurcations. *Journal of Aerosol Medicine* **3**:4, 243-260. [Abstract] [PDF] [PDF Plus]
27. Toshihiko Myojo. 1990. The effect of length and diameter on the deposition of fibrous aerosol in a model lung bifurcation. *Journal of Aerosol Science* **21**:5, 651-659. [CrossRef]
28. B. Asgharian, C. P. Yu. 1990. Deposition of Straight Chain Aggregates in the Human Lung. *Aerosol Science and Technology* **12**:3, 777-785. [CrossRef]
29. Yehia Y. Hammad, Bassam Attieh. 1989. Pulmonary deposition of MMMF. *Journal of Aerosol Science* **20**:8, 1329-1332. [CrossRef]
30. B ASGHARIAN. 1989. Deposition of fibers in the rat lung. *Journal of Aerosol Science* **20**:3, 355-366. [CrossRef]